

Chlorophyll *a* as a measure of seasonal coupling between phytoplankton and the monsoon periods in the Gulf of Oman

Adnan R. Al-Azri · Sergey A. Piontkovski ·
Khalid A. Al-Hashmi · Joaquim I. Goes ·
Helga R. do Gomes

Received: 11 May 2009 / Accepted: 3 December 2009 / Published online: 20 December 2009
© Springer Science+Business Media B.V. 2009

Abstract We present data from a long time-series study to describe the factors that control phytoplankton population densities and biomass in the coastal waters of Oman. Surface temperature, salinity, nutrients, dissolved oxygen, chlorophyll *a* (Chl *a*), and phytoplankton and zooplankton abundance of sea water were measured as far as possible from February 2004 through February 2006, at two stations along the southern coast of the Gulf of Oman. The highest concentrations of Chl *a* (3 mg m^{-3}) were recorded during the southwest monsoon (SWM) when upwelling is active along the coast of Oman. However, results from our study reveal that the timing and the amplitude of the seasonal peak of Chl *a* exhibited interannual variability, which might be attributed to interannual differences in the seasonal cycles of nutrients caused either by coastal upwelling or by cyclonic eddy activity. Monthly variability of SST and concentrations of dissolved nitrate, nitrite, phosphate, and silicate together explained about 90% of the seasonal changes of Chl *a* in the coastal ecosystem of the Gulf of Oman. Phytoplankton

communities of the coastal waters of Oman were dominated by diatoms for most part of the year, but for a short period in summer, dinoflagellates were dominant.

Keywords Monsoon winds · *Noctiluca scintillans* · Zooplankton · Nutrients

Introduction

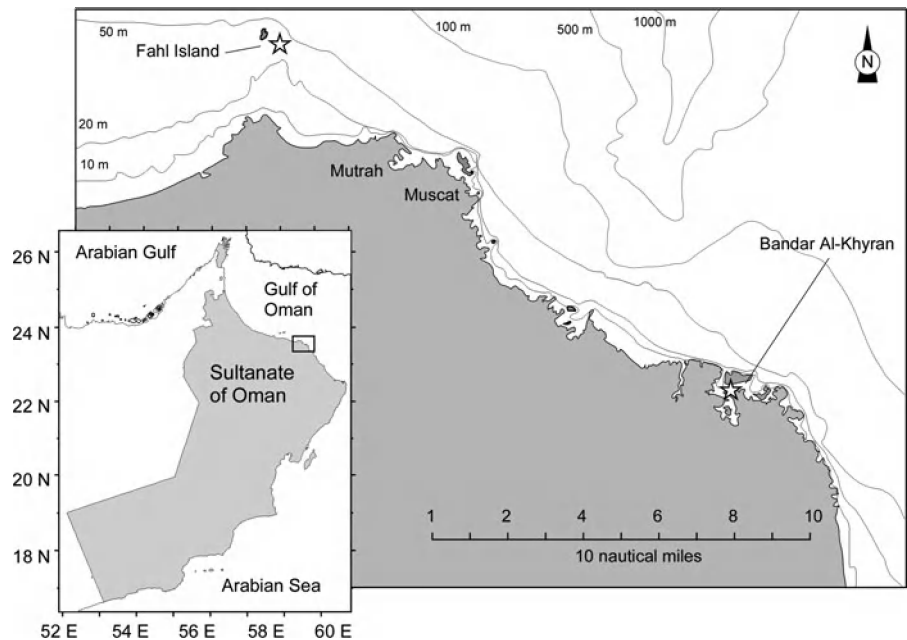
The Sultanate of Oman has an extensive coastline of 3,165 km, which includes the Gulf of Oman (GOO) in the North and the Arabian Sea in the South (Fig. 1). Compared with the extensive research on phytoplankton productivity carried out in the offshore oceanic waters of the Arabian Sea during the International Joint Global Fluxes program (Wiggert et al. 2000; Smith 2001; Marra and Barber 2005), phytoplankton variability in the coastal waters of Oman is poorly known. There is lack of a dedicated program with systematic sampling along the coast at regular time intervals: no information is available on seasonal and interannual variability of phytoplankton communities.

Based on the extensive investigations on the physical and biochemical processes in the Arabian sea, we can infer that physical–biological coupling in the coastal ecosystem of the GOO is largely driven by

A. R. Al-Azri · S. A. Piontkovski (✉) · K. A. Al-Hashmi
College of Agricultural and Marine Sciences,
Sultan Qaboos University, P.O. Box 34,
Al-Khod 123, Sultanate of Oman
e-mail: spiontkovski@gmail.com

J. I. Goes · H. R. do Gomes
Bigelow Laboratory for Ocean Sciences, West Boothbay
Harbor, Boothbay, ME 04575, USA

Fig. 1 Location of sampling stations, Fahal and Bandar Al-Khyran (BK) in the Gulf of coast of Oman. Insert shows the Gulf of Oman and the west coast of the Sultanate of Oman along the Arabian Sea



meteorological forcing, i.e. the monsoons, which manifest themselves as strong, seasonally reversing winds (Wiggert et al. 2000). The monsoons comprise the north east monsoon (NEM) and the south west monsoon (SWM). The NEM extend from November–February, during which sea surface winds over the Gulf of Oman are predominantly northeasterly (Schott et al. 1990), and the SWM extends from June–mid-September when sea surface winds over the region are predominantly from the southwest (Brock and McClain 1992) and stronger than during the NEM (Burkill et al. 1993). During SWM, coastal upwelling persists along the coast of Oman with stronger impacts in the southern part of the coast (Dhofar region; Savidge et al. 1990). The effects of upwelling can extend to about 750 km offshore of Oman and can also be observed in the Gulf of Oman through the injection of cool water that strongly affects temperatures profiles during summer. The extent of intrusion of upwelled water into the Gulf of Oman can be strongly impacted by high air temperature and the inflow of the water from the Persian Gulf, both of which lead to strong vertical stratification in the coastal areas (Quinn and Johnson 1996).

Major goal of this study was to investigate the seasonal cycle of phytoplankton and the extent of coastal physical–biological coupling in the Gulf of

Oman, which supports a large fisheries industry (Al-Jufaili et al. 2006). We present here results based on a 2-year study involving fortnightly sampling of physical, chemical, and biological variables in this poorly studied region.

Methodology

Water samples were collected from a depth of 1 m twice a month when possible, from February 2004 to February 2006, at two stations: Fahal (F, 23.67°N, 58.5°E) and Bandar Al-Khyran (BK, 23.51°N, 58.72°E; Fig. 1). The latter is the largest semi-enclosed bay on the southern end of the Gulf of Oman, with about 4 km² in surface area and an average depth of 10 m. The bay has two inlets and is surrounded by steep rocky hills and cliffs of Permian limestones and shales lined with shallow coral communities. Fahal is located 25 km to the north, with an average depth of 20 m in the sampling region.

Continuous temperature and salinity profiles were measured with an Idronaut-Ocean Seven 316 CTD[®], probe fitted with additional sensors for measuring Chl *a* by fluorescence and the other for dissolved oxygen (DO). Subsurface water samples representative of the mixed layer were collected at 1 m with 5 l Niskin bottles for analyses of nitrate, nitrite, phosphorus, and

silicate. The samples were immediately frozen after collection for analysis in the laboratory. Water samples were later thawed and analyzed for nutrients using a 5-channels SKALAR[®] FlowAccess auto-analyzer according to the procedures described in Strickland and Parsons (1972) and modified by the manufacturer (Skalar analytical, 1996).

Subsamples for Chl *a* (250–1,000 ml) were filtered through 47 mm Whatman GF/F filters, which were then extracted for 24 h into 10 ml of 90% acetone solution under cold and dark conditions for 24 h. Chl *a* concentrations were measured using a Turner 10 Designs Fluorometer according to Tett (1987). Subsamples for phytoplankton abundance were collected in dark glass bottles (50–100 ml) into which 5–10 drops of acid Lugol's solution (Thronsdon 1978) were added and stored at 4°C. The entire sample (50–100 ml) was transferred into graduated cylinders and allowed to settle overnight. The upper layer of seawater in the measuring cylinder was carefully siphoned off using a tube, one tip of which was covered with a 15 µm mesh net to concentrate the sample to 20 ml. The concentrated sample was then transferred into sedimentation chambers to settle overnight before counting using inverted microscopy (Utermohl 1958). Phytoplankton densities were counted by transferring 1 ml replicates of the concentrated sample onto a Sedgewick Rafter counting chamber, and identification was based on standard keys in most cases to the species level.

Zooplankton samples were collected using a Bongo net (mouth surface area: 0.125 m², with a 150 µm mesh sieve: equipped with a Hydrobios[®] digital flowmeter) knot towed obliquely at a speed of one knot from near the bottom to the surface. Samples were transferred to 0.5 l bottles and preserved in 5% borate-buffered formaldehyde for analysis later. In the laboratory, different taxonomic groups were identified to the genus level and if possible to species level and then counted under a stereomicroscope after sub-sampling.

Monthly data on atmospheric pressure (hPa), wind speed (knots), and air temperature (°C) were obtained from the nearest meteorological station in Seeb, about 20 km from the Fahal Island (60 km from Bandar Al-Khyran).

Data on the sea surface altimetry were obtained from the CCAR Global Near Real-Time Sea Surface Anomaly Data Viewer, which allowed to produce

maps from the TOPEX/Poseidon—1/2 altimeter in near real-time. We used the 8 days averaging images to produce the altimetry map.

In addition to Chl *a* measurements, the seasonality of phytoplankton was also studied using Chl *a* from NASA SeaWiFS satellite. Maps of SeaWiFS satellite Chl *a* data (monthly, Level-3, Standard Mapped Image product) are available from NASA's ftp site at <http://oceancolor.gsfc.nasa.gov/ftp.html>. These maps provided information on the timing and the extent of phytoplankton blooms along the Omani coast. Chl *a* concentrations were extracted from monthly, global SeaWiFS images for the region covering F and BK and were compared with those derived from the field.

The NASA database on the Ocean Biogeochemical Model assimilated monthly global products was employed to retrieve time series for sea surface nitrate concentration. Monthly time series used in this study were acquired using the GES-DISC Interactive Online Visualization and Analysis Infrastructure software as part of the NASA's Goddard Earth Sciences Data and Information Services Center.

All time-series data plotted were approximately by cubic spline interpolation. Multiple stepwise regression analysis was used to estimate the contribution of atmospheric pressure, air temperature, SST, salinity, concentrations of NO₃, NO₂, Si, NH₄, and PO₄ on the seasonal cycle of the Chl *a*.

Results

Despite the long distance between the two stations, monthly variations of key parameters such as SST, salinity, phosphate, DO, and Chl *a* did not differ much to justify separate treatment of the data (Table 1). The data presented here thus represent average values over the two sampling sites.

Temperature

In 2004, following a gradual decline of atmospheric pressure from February through mid summer (Fig. 2a), winds achieved their maximal stable speed (6 m s⁻¹) in July and markedly affected fluctuations of the air temperature and SST. There was a clear coupling between the atmosphere and the ocean, as evidenced in the statistically significant relationship between air temperature and atmospheric pressure

Table 1 Results of the nonparametric *t*-test for independent samples from Bhandar Khairan (BK) and Fahal (F)

Parameter	<i>t</i> -Value	Degree of freedom	Probability	<i>F</i> -ratio
SST (F) vs. SST (BK)	−0.12	86	0.90	1.02
Oxygen (F) vs. oxygen (BK)	−1.91	86	0.06	1.19
Phosphates (F) vs. phosphates (BK)	−1.66	86	0.10	1.57
Chlorophyll <i>a</i> (F) vs. chlorophyll <i>a</i> (BK)	−0.22	86	0.83	1.07

Note: the above pairs were treated as dependent samples

Fig. 2 Monthly variation averaged over the two sampling regions.

a Atmospheric pressure (hPa, *solid line*) and wind speed (m s^{-1} , *dotted line*).
b Atmospheric temperature ($^{\circ}\text{C}$, *dashed line*), sea surface temperature ($^{\circ}\text{C}$, *solid line*), and dissolved oxygen concentration (ml l^{-1} , *dotted line*)

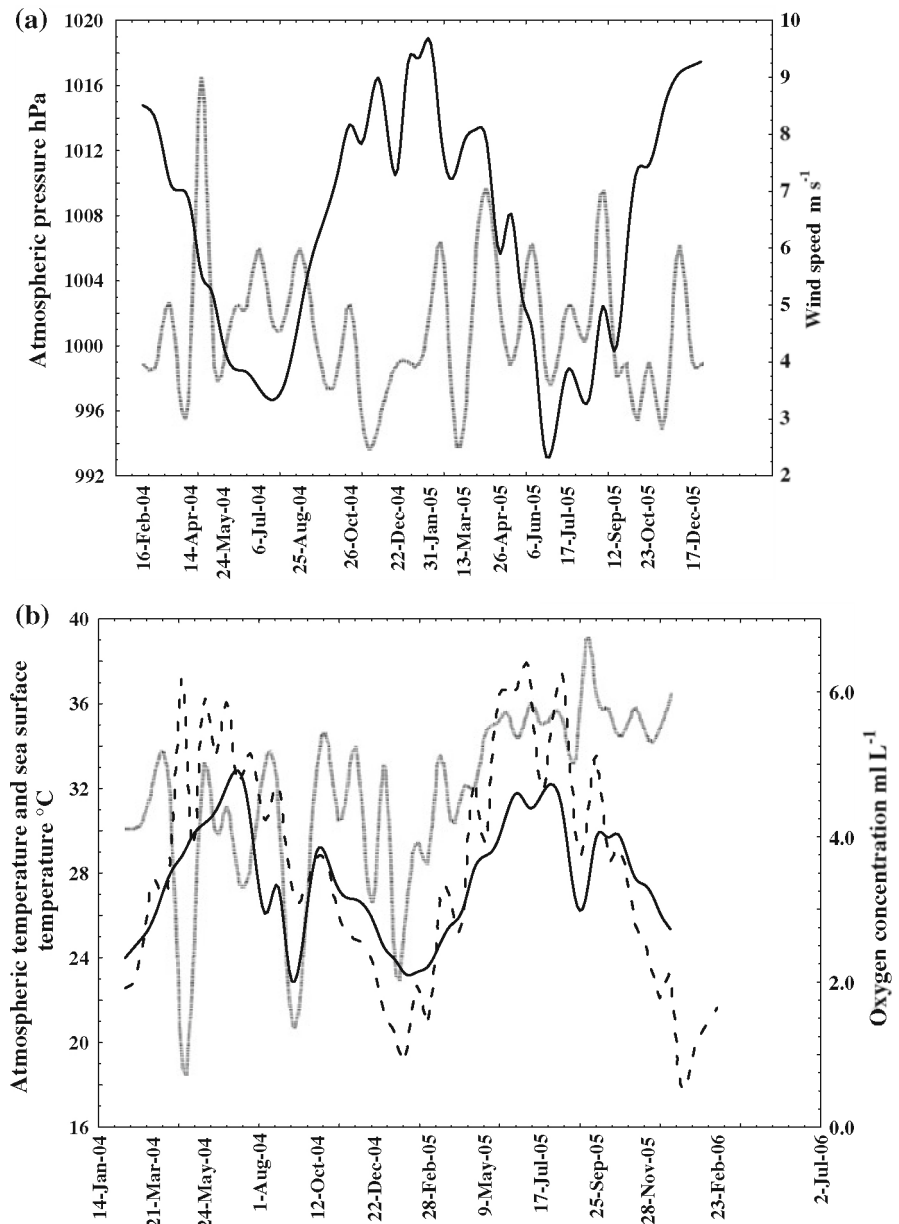
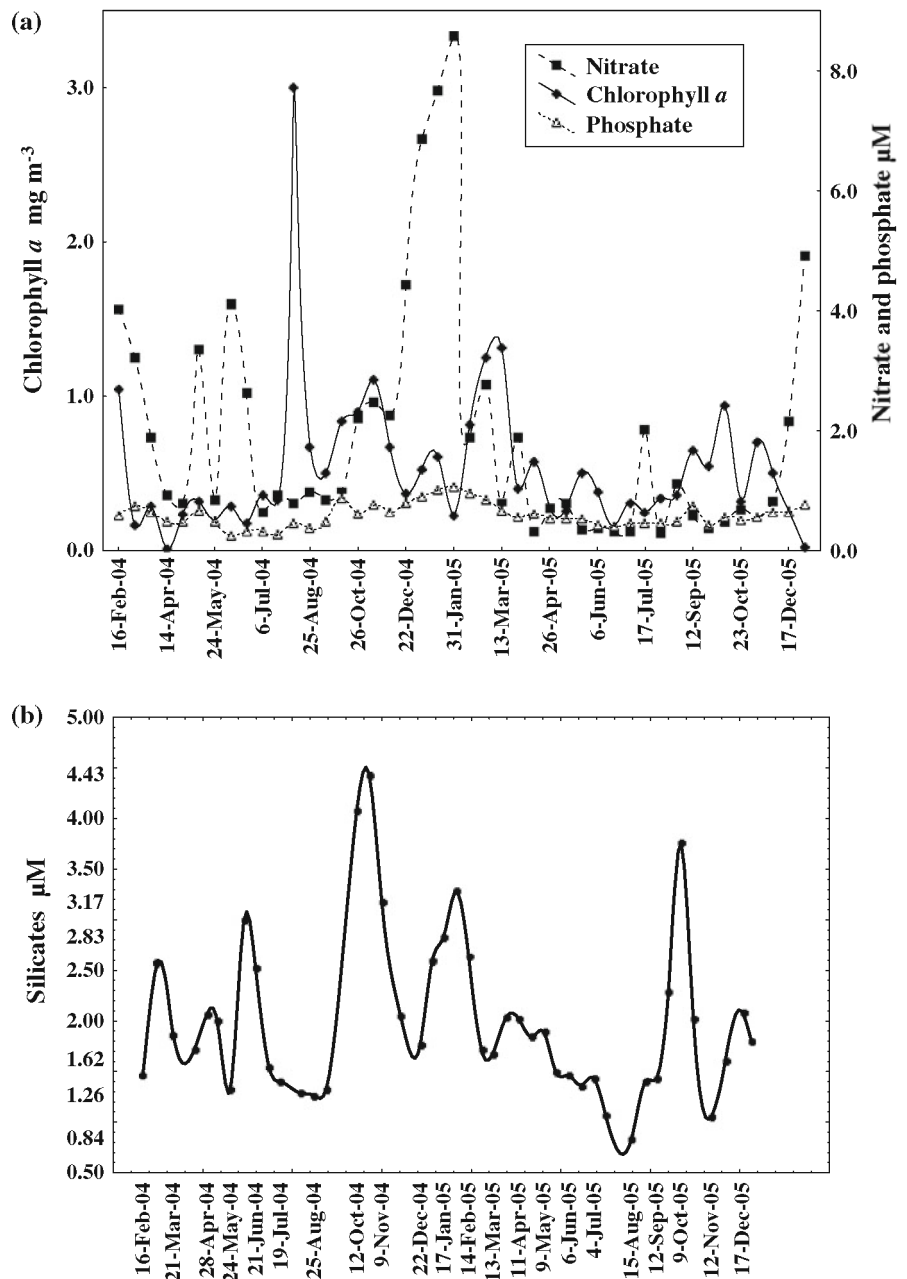


Fig. 3 Monthly variation averaged over the two sampling regions. **a** Chl *a*, nitrate, and phosphate; **b** Silicate



($r = -0.73$, $P < 0.01$) as well as between air temperature and SST ($r = 0.84$, $P < 0.01$). Average SSTs ranged between 24 and 32°C with the maximal value during summer and a minimum in winter. During the summers of 2004 and 2005, the most significant decline (~ 6 – 10°C) in SST was experienced during August and September of both years (Fig. 2b). Although this pattern of decline was

consistent during the 2 years of sampling, the SWM of 2004 was much cooler than the SWM month of 2005. The other component of the SST decline pertains to seasonal winter cooling and convective mixing, with minimal SST values observed in January (Fig. 2b). Seawater salinity showed seasonal changes which were analogous to that of SST ($r = 0.68$, $P < 0.05$).

Dissolved oxygen

Fluctuations of DO concentrations were greater in 2004 than in 2005 (Fig. 2b). Monthly changes in DO in 2004, exhibited a multimodal type of distribution, exhibiting hypoxic conditions twice, concentrations decreasing to 0.6–0.9 ml l⁻¹ in April and 1.7 ml l⁻¹ in September. Surprisingly, the lower DO concentrations in April 2004 were associated with warmer waters of 28.5°C compared with cooler waters (23.3°C) in September (Fig. 2b).

Inorganic nutrients

The seasonal variations of nutrient followed a strong seasonal trend, with high concentrations in February 2004 and January 2005 for all nutrient except silicate that peaked in October in both years (Fig. 3a, b). The nitrate varied much more than phosphate (Fig. 3a). Concentrations of nitrate varied between 8.7 µM in January to <2.0 µM during summer. Phosphate followed a similar trend to nitrate with the highest concentrations 1.0 µM in January of 2005 and lower concentrations during summer for both years. Maxima for silicate for both years were 4.5 and 3.5 µM, in October 2004 and October 2005, respectively. Silicate minimum occurred during summers, with the lowest concentrations (0.7 µM) during summer 2005.

Chlorophyll *a*

Chl *a* concentrations exhibited a major peak in August (3 mg m⁻³) during the SWM and a second smaller one in March (1.3 mg m⁻³) during the NEM. Chl *a* concentrations extracted from SeaWiFS data for the region were consistent with the field measurements and confirmed that the Chl *a* peak reflected the period when coastal upwelling produced conditions for the SWM phytoplankton bloom that extended to almost entire western Arabian Sea (Figs. 3, 4, 5). The SWM peak (0.95 mg m⁻³) in Chl *a* in 2005 had shifted to October and was not as prominent as in August 2004.

The map of the sea surface height anomalies (Fig. 6) showed that in the beginning of September, the coastal zone between two sampling sites could have been influenced by the local divergence of waters induced by the cyclonic eddy that transported the offshore oxygen minimum (from the depths of

about 40–60 m) and impinged it on the coast. Indeed, the monthly time series of the oxygen (vertical profiles; Fig. 7) indicated the persistence of water masses with depleted oxygen in which the concentration was 10–15% the values observed before and after eddy passage through the region. The same event was observed in the time series of Chl *a* profiles. The patches of Chl *a* were mostly pronounced in the upper 10 m layer, throughout study period.

Statistical relationships between Chl *a* and environmental parameters were assessed using a multiple regression analysis of the median smoothed monthly series of wind sea surface pressure, air temperature, SST, salinity, oxygen, NO₃, NO₂, SiO₃, NH₄, and PO₄ concentrations. The regression analysis showed that the above parameters explained 91% of the Chl *a* seasonal variability (Table 2).

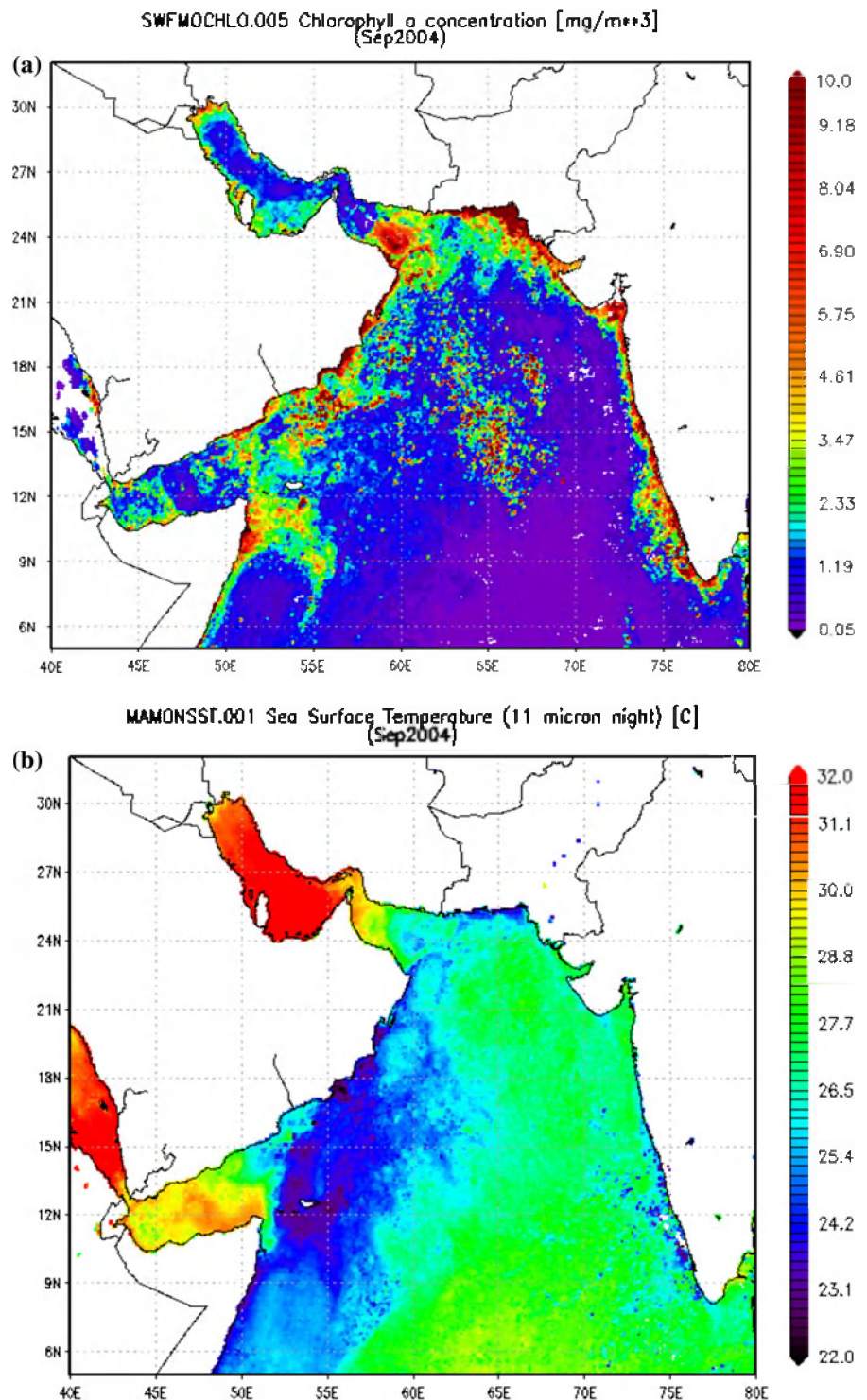
Phytoplankton

Taxonomic analysis of phytoplankton provided insights into biological components that contributed to the variations of Chl *a*. In general, the phytoplankton communities at our study sites were dominated by diatoms (Table 3) especially in January and February, when the annual diatom-to-dinoflagellate abundance ratio reached about 10. While diatoms dominated in winter, dinoflagellate did so in summer. The study period maximum for phytoplankton (97 360 cells/dm⁻³) was recorded in February 2004 at station F, with *Leptocylindricus* sp. comprising 93%. During late winter and early spring, the heterotrophic dinoflagellate *Noctiluca scintillans* accounted for a significant fraction of the total phytoplankton abundance. Cyanobacteria were less abundant and occurred during summer at both stations when nitrate concentrations were below 1 µM.

Zooplankton

We began sampling zooplankton in June 2005, which made phytoplankton and zooplankton time series only partly compatible. The zooplankton total abundance was dominated by copepods at both stations (~80%). From June 2005 through February 2006, monthly variation of the copepod percentage was fairly small. For example, for the zooplankton

Fig. 4 Spatial distribution of chlorophyll *a* and sea surface temperature for the first week of September, 2004 (The SeaWiFS data. Map produced by Giovanni software). **a** Chlorophyll *a*, mg m^{-3} . **b** Sea surface temperature, $^{\circ}\text{C}$



fraction collected by the 150 μm net, the variation coefficient of the copepod percentage was 13 and 16%, for the BK and F stations accordingly.

In terms of taxonomy, the copepods were represented by 29 families and about 50 species of which most abundant species were *Temora turbinata*,

Fig. 5 Monthly variation of chlorophyll *a* (mg m^{-3}) in the Gulf of Oman. **Bold line** indicates sampled chlorophyll, BK + F stations. **Dashed line** indicates oceanic region of the Gulf of Oman ($24\text{--}25^\circ\text{N}$, $59\text{--}60^\circ\text{E}$), MODIS Aqua sensor. **Solid line** indicates coastal region ($23\text{--}24^\circ\text{N}$, $57\text{--}58^\circ\text{E}$), MODIS Aqua sensor

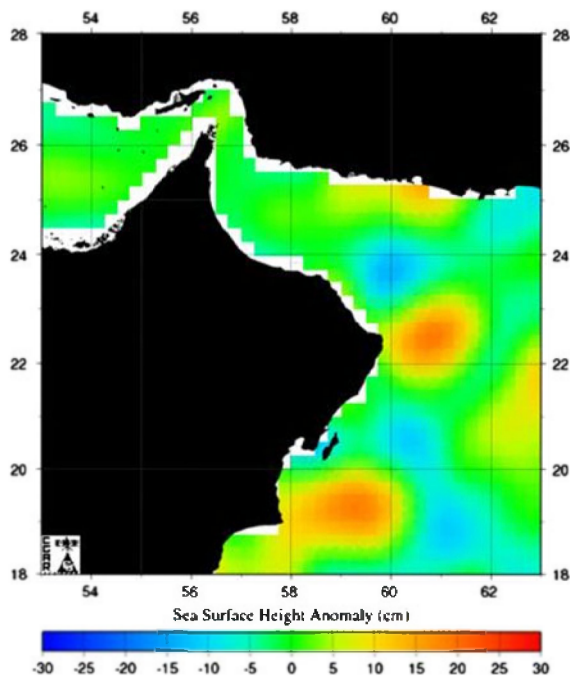
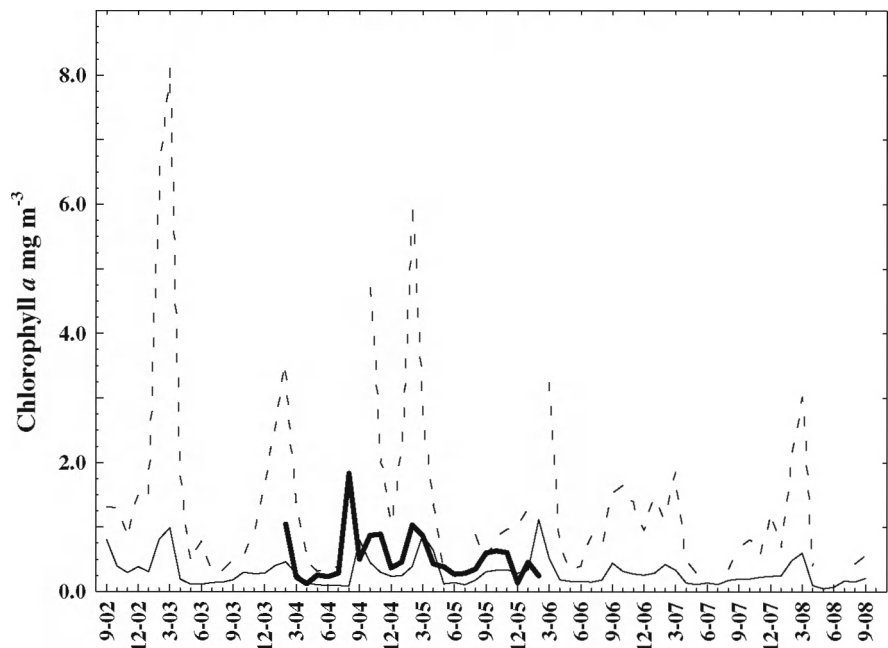


Fig. 6 Sea surface height anomalies for the beginning of September, 2004. (TOPEX/Poseidon—1/2 altimeter. Map produced by the CCAR Real-time Altimeter Data Research Group)

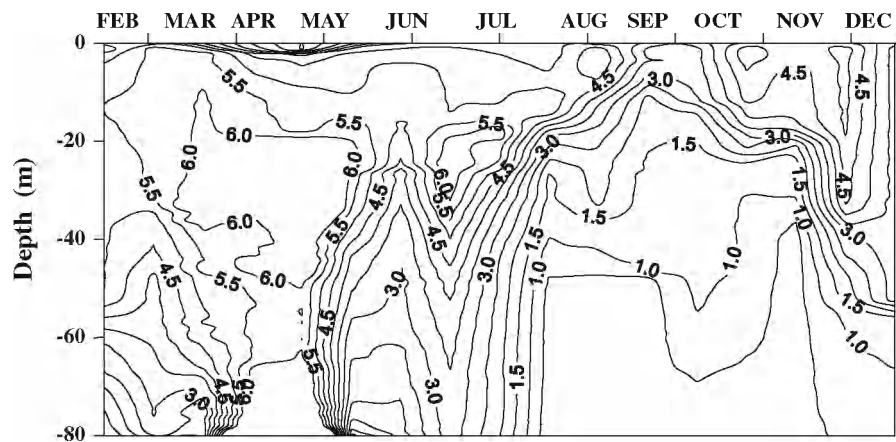
Parvocalanus elegans, *Oithona nana*, *Oithona brevicornis*, and *Centropages orsinii*. The copepod total abundance has reached its maximum in mid

December, at both sampling sites. It should be noted, however, that zooplankton sampling did not cover the annual cycle in full. Among the other taxonomic groups, the cladoceran species (*Penilia avirostris*) and nauplia of Cirripedia were also present in large numbers at both stations.

The next most abundant zooplankton organisms (acting as potential copepod predators) were the chaetognaths. Seasonal variations of the copepod and chaetognath abundance were positively correlated ($r = 0.38$, $P < 0.05$ for BK; $r = 0.32$, $P < 0.05$ for F) pronounced at both sampling regions (Fig. 8). In some way, this correlation reflects the monthly resembled pattern of predator–prey relationship in the coastal waters. Obviously, fluctuations of the chaetognaths abundance are well tuned to the fluctuations of copepods contributing much into the chaetognaths food spectrum (Gray 1961).

Discussion

Our data represent the longest continuous measurements carried out in the coastal waters of Oman. Weather conditions were characteristically rough during the SWM (Thangaraja 1995) due to intensive wind activity, which impeded continuous measurements of the physical, chemical, and biological characteristics along the Omani coast.

Fig. 7 Oxygen profile at OFF station**Table 2** Results of multiple regression analysis ($r = 0.95$, $r^2 = 0.91$; $F = 26.8$, $P < 0.01$) between chlorophyll *a* and physical–chemical variables

Variable	Beta	Beta standard error	St	<i>P</i> value
Wind P	−0.547	0.341	−1.605	0.120
Air T	0.514	0.482	1.067	0.296
SST	−2.592	0.429	−6.035	0.000
Salinity	−0.036	0.165	−0.219	0.828
Oxygen	1.277	0.357	3.580	0.001
NO ₃	−1.011	0.328	−3.086	0.005
NO ₂	1.715	0.412	4.163	0.000
NH ₄	−0.243	0.194	−1.250	0.222
PO ₄	−1.772	0.383	−4.620	0.000
SI	1.074	0.192	5.604	0.000

The coefficients of the regression slope (Beta) and the Student Test (St) with *P* values in bold for parameters that are statistically significant are shown

Wind P atmospheric pressure, Air T atmospheric temperature, SST sea surface temperature, NO₃ nitrate, NO₂ nitrite, NH₄ ammonia, PO₄ phosphate, and SI silicates

Statistical correspondence in the time series of SST, salinity, phosphate, oxygen, and Chl *a* between the two sampling sites positioned 25 km apart indicates that the spatial–temporal scale of the processes influencing variability of physical, chemical, and biological parameters within the study areas can exceed tens of kilometers. For instance, this could be seen through eddies dispersal in the Gulf of Oman and the spatial distribution of sea surface temperature and Chl *a* (Fig. 4).

The most distinct variations in SST are the sharp drops observed in August and July, as also observed

by Coles and Seapy (1998) and Claereboudt et al. (2001) who attributed this to the upwelling and cyclonic eddies that cause, deeper nutrient-rich waters to shoal maybe responsible for the abrupt decreases in SST during SWM. Indeed, SST exhibited significant negative correlation with the sea surface atmospheric pressure ($r = -0.72$, $P < 0.01$). On the other hand, the 2-week drops of temperature were seen in association with minimal steric heights indicating mesoscale impulses of the upwelled water. The influx of deeper, colder waters, and the transport of these offshore oxygen-depleted waters into the coastal shelf region were also responsible for the development of hypoxic conditions at the two stations.

In oceanic waters of the western Arabian Sea, the seasonal cycle of Chl *a* is dominated by two periods of high concentrations, August–September and January–February. These months correspond to the end of the SWM and NEM (Banse and English 2000; Marra and Barber 2005). In our study, the timing and the amplitude of the Chl *a* seasonal peak varied during the study years 2004 and 2005. Peak Chl *a* values of 3 mg m^{−3} recorded in August 2004 were not observed in 2005. Al-Hashmi et al. 2009 (in press) also recorded Chl *a* of 2.7 mg m^{−3} in 2002 in July suggesting interannual differences in both the timing of phytoplankton blooms and their intensity during the SWM.

Of all the parameters that we measured, the seasonal and interannual variability in Chl *a* appeared to be the most significant, followed by DO concentrations and inorganic nutrient (nitrate, nitrite, phosphate, and silicate). In combination, these environmental

Table 3 List of dominant phytoplankton species

Months	Genera	F (%)	BK (%)
February	<i>Chaetoceros</i> sp.		22
	<i>Nitzschia longissima</i>		17
	<i>Leptocylindricus</i> sp.	93	25
	<i>Gymnodinium</i> sp.		10
	<i>Noctiluca scintillans</i>	19	
	<i>Dinophysis caudata</i>	25	
	<i>Prorocentrum triestinum</i>		27
	<i>Protoperidinium quinquecorne</i>		11
	<i>Prorocentrum micans</i>	16	
March	<i>Gonyaulax</i> sp.	29	31
	<i>Prorocentrum micans</i>	11	10
	<i>Scripsiella</i> sp.		20
	<i>Chaetoceros</i> sp.		23
April	<i>Nitzschia</i> sp.	24	
	<i>Protoperidinium depressum</i>	11	
	<i>Prorocentrum micans</i>		37
	<i>Nitzschia</i> sp.	41	
	<i>Gonyaulax</i> sp.		19
	<i>Gymnodinium sanguineum</i>		10
	<i>Noctiluca scintillans</i>	33	
	<i>Prorocentrum compressum</i>	44	24
	<i>Scripsiella</i> sp.		10
May	<i>Coscinodiscus</i> sp.	11	
	<i>Leptocylindricus</i> sp.	11	
	<i>Ceratium dens</i>	10	
	<i>Ceratium furca</i>	10	
	<i>Gymnodinium (heterotrophic)</i>	17	
	<i>Nitzschia</i> sp.	3	94
	<i>Rhizosolenia</i> sp.	13	
	<i>Gonyaulax polygramma</i>	21	10
	<i>Gyrodinium</i> sp.	24	
	<i>Protoperidinium quinquecorne</i>		10
	<i>Plagiotropis</i> sp.	14	10
	<i>Skeletonema</i> sp.		85
June	<i>Spiraulax</i> sp.	16	
	<i>Chaetoceros</i> sp.	12	78
	<i>Rhizosolenia</i> sp.	16	10
	<i>Noctiluca scintillans</i>	40	
	<i>Thalassiosira sackati</i>	10	
July	<i>Ceratium furca</i>	36	
	<i>Protoperidinium depressum</i>	18	
	<i>Chaetoceros</i> sp.		30
	<i>Nitzschia</i> sp.		14
	<i>Rhizosolenia</i> sp.		26

Table 3 continued

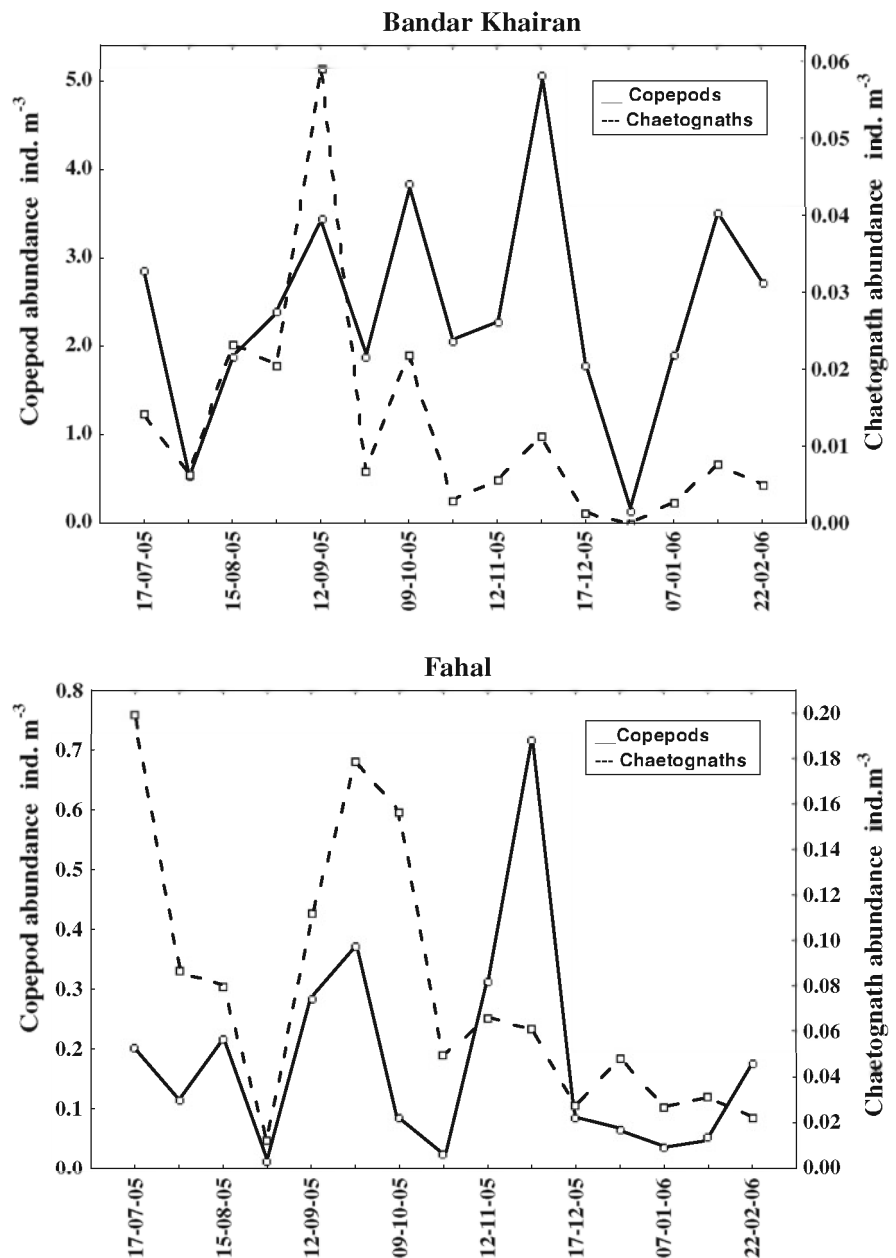
Months	Genera	F (%)	BK (%)
August	<i>Biddulphia</i> sp.	21	
	<i>Coscinodiscus</i> sp.	16	
	<i>Hemidiscus</i> sp.	24	
	<i>Leptocylindricus</i> sp.		21
	<i>Rhizosolenia stolterfothii</i>		13
	<i>Rhizosolenia stigerai</i>		61
September	<i>Noctiluca scintillans</i>	51	
	<i>Chaetoceros coarctatus</i>	12	
October	<i>Ceratium furca</i>	10	12
	<i>Dinophysis caudata</i>	17	
	<i>Gymnodinium</i> sp.	38	12
	<i>Leptocylindricus</i> sp.		16
	<i>Lauderia</i> sp.		13
	<i>Rhizosolenia stolterfothii</i>		27
	<i>Thalassiothrix</i> sp.	13	11
	<i>Ceratium furca</i>	13	12
	<i>Noctiluca scintillans</i>		12
	<i>Protoperidinium</i> sp.	13	14
November	<i>Corethron</i> sp.		60
	<i>Hemidiscus</i> sp.	17	
	<i>Nitzschia</i> sp.	13	
	<i>Thalassionema nitzschoides</i>	13	
	<i>Amphisolenia</i> sp.	12	
	<i>Ceratium fusus</i>	24	
	<i>Gonyaulax</i> sp.	12	
	<i>Protoperidinium</i> sp.	12	11
	<i>Rhizosolenia stolterfothii</i>		77

variables explained about 90% of the seasonal changes of Chl *a*. Changes in SST were clearly the result of fluctuations in atmospheric pressure and changes in the intensity of sea surface winds.

The seasonal cycle of Chl *a* can lag behind the cycle of nutrient by up to few months. For example, the cross-correlation analysis for the monthly time series (1997–2006), showed that Chl *a* increase usually followed SST decrease with the time lag ranging from zero to 2 months ($P < 0.05$). Such a correlation was also evident between remotely sensed Chl *a* and remotely sensed nitrates (Fig. 9).

Coastal mixing and advective transport are other possible processes impacting variations in Chl *a* and physical–biological coupling along the coast of Oman. In the western Arabian Sea, a major part of

Fig. 8 Monthly variation of the total copepod and chaetognath abundance for the BK and F sampling sites



the energy supporting the currents is attributed to the mesoscale processes as eddies and meandering of currents (Banse and Piontkovski 2006; Gomes et al. 2008). Mesoscale eddies are most active during the SWM, in particular in the northwestern part of the Arabian Sea (Swallow 1984; Madhupratap et al. 1996; Gomes et al. 2008). For instance, current meter data showed that in the Omani waters, over 90% of the total kinetic energy was associated with the eddy field (Flagg and Kim 1998).

In our coastal measurements, the sudden drops in sea surface temperature and oxygen concentration in the middle of September 2004 (Fig. 2b) could have been associated with the persistence of cyclonic eddy that approached the sampling region in the beginning of September (Fig. 6).

The UK JGOFS transects with sampling stations directed off the Omani coast revealed a substantial decline of Chl *a* concentration toward the open sea (Barlow et al. 1999). Thus, through the transport

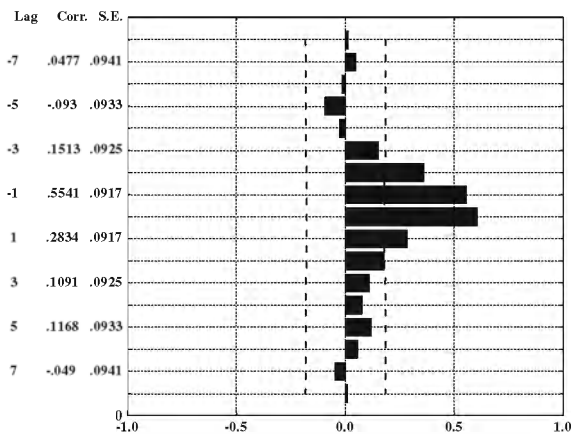


Fig. 9 Cross-correlation function for the SeaWiFS monthly time series (1997–2006) of chlorophyll *a* (lagged) and nitrates. Y-axis dashed line indicates 95% confident limits. Lag the lag time in months, Corr correlation coefficient, and SE standard error for correlation coefficient (with values on X-axis)

along the gradient, meanders of coastal currents and propagating eddies could decrease or increase the values of physical, chemical, and biological characteristics. For instance, the annual average for concentration of the Chl *a* at station F, exceeded the concentration 1.3 times that we measured 5 km offshore.

In synthesizing the JGOFS data, Marra and Barber (2005) concluded that in the western Arabian Sea phytoplankton is not limited by either irradiance or nutrient supply. Throughout the sampling period, even during the SWM, light levels were adequate for phytoplankton growth. The major control on phytoplankton biomass in their work appeared to be mesozooplankton whose grazing on phytoplankton populations was high (Banse 1992, 1994).

In our study, the situation seem to be different, where nutrient and DO explained major part of monthly variability of Chl *a*. We do not rule out the role of mesozooplankton in controlling phytoplankton biomass; however, the lack of information on assessment of zooplankton grazing rates, along with relatively short times series of zooplankton and phytoplankton in our study had limitation in explaining the interaction of zooplankton and phytoplankton.

Overall, the evolution of the phytoplankton community, characterized by a short dominance of dinoflagellates and greater abundance of diatoms throughout the year, and that of the herbivorous copepod species and their consumers (chaetognaths

and jellyfish species) implied that the classical trophic chain is fairly well developed in the coastal ecosystem of the Gulf of Oman.

Conclusion

Monthly variability of sea surface temperature, and concentration of dissolved oxygen, nitrates, nitrites, phosphates, and silicates statistically explained about 90% of the seasonal changes of Chl *a* in the coastal ecosystem of the Gulf of Oman (Muscat region). In 2004–2005, the highest concentrations of Chl *a* were associated with the SWM season. However, the timing and the amplitude of the Chl *a* seasonal peak exhibited interannual changes. These changes might be due to interannual differences in the seasonal cycles of nutrient. The eddies passing through the region could have also impacted intraseasonal (monthly) variability in Chl *a* and physical–chemical characteristics.

Acknowledgments This work was supported by the research grants from the Sultan Qaboos University (IG/AGR/FISH/04/03; IG/AGR/FISH/09/02) and the Ministry of Fisheries Wealth (Sultanate of Oman). This work was also supported by Grants NNG04GH50G, NNG04GM64G and NNH08ZDAOOIN from the National Aeronautical and Space Agency (NASA), the National Science Foundation (NSF), USA to JIG and HRG. We acknowledge Gene Feldman, C.R. McClain and others at the NASA Goddard Space Flight Center Ocean Color Web for the Chlorophyll product. Additional analyses used in this study were produced with the Giovanni online data system, developed and maintained by the NASA GES DISC.

References

- Al-Hashmi KA, Claereboudt M, Al-Azri AR, Piontkovski SA (2009) Seasonal changes of chlorophyll “a” and environmental characteristics in the gulf of Oman. *Open Mar Biol J* (in press)
- Al-Jufaili SM, Al-Azri AR, Al-Shuaili SS (2006) A preliminary investigation on the Omani sardines and anchovies stock fluctuation; recommendations for future studies. *Pak J Biol Sci* 9(6):1073–1082
- Banse K (1992) Grazing, the temporal changes of phytoplankton concentrations, and the microbial loop in the open sea. In: FALKOWSKI P, Woodhead AD (eds) *Primary productivity and biogeochemical cycles in the sea*. Plenum Press, New York, pp 409–440
- Banse K (1994) Grazing and zooplankton production as key controls of phytoplankton production in the open ocean. *Oceanography* 7:13–20

- Banse K, English DC (2000) Geographical differences in seasonality of CZCS-derived phytoplankton pigment in the Arabian Sea for 1978–1986. *Deep-Sea Res II* 47:1623–1677
- Banse K, Piontkovski SA (eds) (2006) The mesoscale structure of the epipelagic ecosystem of the open northern Arabian Sea. Universities Press, Hyderabad, p 248
- Barlow RG, Mantoura RFC, Cummings DG (1999) Monsoonal influence on the distribution of phytoplankton pigments in the Arabian Sea. *Deep-Sea Res* 46(3–4):677–701
- Brock JC, McClain CR (1992) Interannual variability in phytoplankton blooms observe in the northwestern Arabian Sea during the southwestern monsoon. *J Mar Res* 97(C1):733–750
- Burkill PH, Mantoura RFC, Owens NJP (1993) Biogeochemical cycling in the northwestern Indian Ocean: a brief overview. *Deep-Sea Res II* 40(3):643–649
- Claereboudt M, Hermosa G, McLean E (2001) Plausible cause of massive fish kill in the Gulf of Oman. In: Proceeding of the first international conference on Fisheries, Aquaculture and Environments in the Northwest Indian Ocean, vol 2. SQU, Oman, pp 123–132
- Coles SL, Seapy DG (1998) Ultra-violet absorbing compounds and tumorous growths on acroporid corals from Bandar Khayran, Gulf of Oman, Indian Ocean. *Coral Reefs* 17:195–198
- Flagg C, Kim HS (1998) Upper ocean currents in the northern Arabian Sea from shipboard ADCP measurements collected during 1994–1996 US JGOFS and ONR programs. *Deep-Sea Res II* 45:1917–1959
- Gomes HR, Goes JJ, Matondkar P, Sushma GP, Al-Azri AR, Prasad GT (2008) *Noctiluca miliaris* in the Arabian Sea. An in situ and satellite study. *Deep-Sea Res I* 55:751–765
- Gray P (1961) Encyclopedia of biological science. Reinhold, New York
- Madhupratap M, Gopalakrishnan TC, Haridas P, Nair KKC, Aravindakshan PN, Padmavati G, Sheney P (1996) Lack of seasonal and geographic variation in mesozooplankton biomass in the Arabian Sea and its structure in the mixed layer. *Curr Sci In* 71:863–868
- Marra J, Barber RT (2005) Primary productivity in the Arabian Sea: a synthesis of JGOFS data. *Prog Oceanogr* 65(2–4):159–175
- Quinn NJ, Johnson DW (1996) Cold water upwelling cover Gulf of Oman. *Coral Reefs* 15:214
- Savidge G, Lemon J, Matthews AJ (1990) A shore-based survey of upwelling along the coast of Dhofar region, southern Oman. *Continent Shelf Res* 10:259–275
- Schott F, Swallow JC, Fieux M (1990) The Somali Current at the equator: annual cycle of currents and transports in the upper 1000 m and connection with neighbouring latitudes. *Deep-Sea Res* 37:1825–1848
- Smith SL (2001) Understanding the Arabian Sea: reflections on the 1994–1996 Arabian Sea Expedition. *Deep-Sea Res* 48(II):1385–1402
- Strickland J, Parsons T (1972) A practical handbook of seawater analysis. Bulletin 167, 2nd edn. Fisheries Research Board Canada, Ottawa, Canada, 310 pp
- Swallow J (1984) Some aspects of the physical oceanography of the Indian Ocean. *Deep-Sea Res* 31:639–650
- Tett P (1987) Plankton. In: Baker JM, Wolff WJ (eds) Biological surveys of estuaries and coasts. Cambridge University Press, Cambridge, pp 328–335
- Thangaraja M (1995) Hydro-biology of Oman. MSFC research report no. 95-1. Ministry of Agriculture and Fisheries. Muscat, 153 pp
- Thronsdon J (1978) Preservation and storage. In: Sournia A (ed) Monographs on oceanographic methodology 6: phytoplankton manual. United Nations Educational, Scientific and Cultural Organisation (UNESCO), Paris
- Utermohl H (1958) Zur Vervollkommung der quantitativen Phytoplankton Methodik. *Mitt Int Ver Limnol* 9:1–38
- Wiggert JD, Jones BH, Dickey TD, Brink KH, Weller RA, Marra J, Cadispoli LA (2000) The northeast monsoon's impact on mixing, phytoplankton biomass and nutrient cycling in the Arabian Sea. *Deep-Sea Res* 47:1353–1386